Proc. Natl. Acad. Sci. USA
Vol. 83, pp. 7736–7740, October 1986
Biophysics

Local Fe site structure in the tense-to-relaxed transition in carp deoxyhemoglobin: A XANES (x-ray absorption near edge structure) study

(hemoprotein structure)

A. BIANCONI[†], A. CONGIU-CASTELLANO[†], M. DELL'ARICCIA[†], A. GIOVANNELLI[†], S. MORANTE[‡], E. BURATTINI[§], AND P. J. DURHAM[¶]

[†]Dipartimento di Fisica, Universitá "La Sapienza," 00185 Roma, Italy; [‡]Dipartimento di Fisica, Universitá di Roma II, 00173 Roma, Italy; [§]Consiglio Nazionale delle Ricerche–INFN Laboratori Nazionali di Frascati, 00044 Frascati, Italy; and [¶]Science and Engineering Research Council, Daresbury Laboratory, Daresbury, Warrington WA4 4AD, United Kingdom

Communicated by Hans Frauenfelder, May 14, 1986

ABSTRACT **The Fe-site structure variation in the transition from the low-affinity tense (T) quaternary structure to the high-affinity relaxed (R) structure in carp deoxyhemoglobin was studied by analysis of multiple scattering resonances in the XANES (x-ray absorption near edge structure) spectra. High signal-to-noise XANES spectra were measured at the Frascati "wiggler" synchrotron radiation facility. We find that the forces on the Fe active site due to the change of quaternary protein conformation do not induce (*i*) variations >0.01 Å in interatomic Fe–N distances, (*ii*) variations >0.1 Å in the Fe displacement toward the heme plane, or (*iii*) the "doming" of the heme. The relevance of these results to the mechanism of protein control of ligand binding is discussed.**

Below pH 5.6 in the presence of allosteric effectors like inositol hexakisphosphate (Ins-P_6), carp hemoglobin has a very low oxygen affinity and ligand binding is not cooperative (1–4). This lack of cooperativity has been attributed (5) to the inhibition at acid pH of the allosteric transition from the tense (T) conformation of carp deoxyhemoglobin to the relaxed (R) conformation with ligand binding. On the other hand, the transition, with release of the ligand, from the R conformation of the ligated carp hemoglobin (HbCO and HbN_3) to the T conformation of deoxyhemoglobin is precluded at alkaline pH. Therefore, carp deoxyhemoglobin presents the anomalous R conformation with high ligand affinity at alkaline pH that we will call here R_d. (Similarly, T_d is the T quarternary state of carp deoxyhemoglobin at low pH.)

Because allosteric effectors can induce the T_d (low affinity) to R_d (high affinity) transition in carp deoxyhemoglobin, this protein has attracted much interest with the aim of investigating the correlation between the protein quaternary conformation and the local structure in the active site—i.e., the Fe position in the heme, which is a key point in the explanation of oxygen-binding cooperativity in hemoproteins (6, 7). The interest is now addressed to the correlation between the variation of the quaternary structure (defined as the structure of the α_1/β_2 interface) and the conformation of the immediate environment about the Fe site (which defines the protein tertiary structure) and the Fe coordination site structure.

Diffraction studies to establish at the same time the protein conformation and local structure of the active site can be performed only on protein crystals. Spectroscopic methods that can be used to study the protein in solution, such as optical spectroscopy, resonance Raman spectroscopy, and magnetic susceptibility, are not direct probes of atomic positions.

The structure of carp deoxyhemoglobin, as well as its variation from the low- to high-affinity form, has not been determined by crystallography. Therefore, there is a lack of direct experimental information on the variation of structure of this protein. Small changes have been observed in resonance Raman spectra between low-affinity deoxyhemoglobin and anomalous or pathological high-affinity hemoglobins (8–11). Time-dependent resonance Raman studies of transient hemoglobin species have found quaternary structure-dependent forces on the Fe–histidine bond, which have been assigned to a tilt of the proximal histidine (12). The resonance Raman spectra (13, 14) show a frequency shift of the iron-histidine stretching mode Fe–N_ϵ (His F8) in the $T_d \rightarrow R_d$ transition in carp deoxyhemoglobin. In a nuclear magnetic resonance (NMR) study of carp deoxyhemoglobin (15), an increase in the proximal histidine imidazole ring NH hyperfine shift, attributed to a strengthening of the Fe-histidine bond in the $T_d \rightarrow R_d$ transition, has been observed.

Recent NMR investigation (16) on the conformation differences between carp and human adult hemoglobin indicate that the two proteins differ in tertiary and quaternary structure, but the functional significance of this alteration is unclear. Moreover, the NMR spectra of carp deoxyhemoglobin at low pH (low affinity) and carp HbCO plus Ins-P_6 (low affinity) show a proton resonance that could be attributed to a T quaternary structure and that is absent in the spectra of carp deoxyhemoglobin at high pH (high affinity) and carp HbCO without Ins-P_6 (high affinity).

In the work described here, we have used XANES (x-ray absorption near edge structure) spectroscopy (17–22) to investigate the local structure changes around the Fe ion in the heme pocket induced by the $T_d \rightarrow R_d$ transition in the deoxy form.

In the XANES energy range, some tens of electronvolts (1 eV = 1.602×10^{-19} J) above the absorption threshold, the absorption cross section is modulated by the scattering of the photoelectron, emitted at the absorbing atom (Fe), by neighboring atoms. In the XANES, the photoelectron is in the multiple scattering regime. All the multiple scattering pathways with $n \geq 2$ scattering events which begin and end on the Fe site at the origin contribute to XANES. It is via multiple scattering that XANES probes higher-order correlation functions of atomic spatial distribution—i.e., bonding angles. In particular by means of XANES spectroscopy, we have been able to measure the displacement of the iron out of the

The publication costs of this article were defrayed in part by page charge payment. This article must therefore be hereby marked "*advertisement*" in accordance with 18 U.S.C. §1734 solely to indicate this fact.

Abbreviations: XANES, x-ray absorption near edge structure; EXAFS, extended x-ray absorption fine structure; Ins-P_6, inositol hexakisphosphate.

porphyrin plane in deoxy hemoproteins (23, 24), and the bonding angle of the ligands (25–27).

At higher energies in x-ray absorption spectra, the photoelectron enters in the single-scattering, EXAFS (extended x-ray absorption fine structure) regime, where only the pair correlation function is probed. EXAFS therefore provides bond distances.

Because EXAFS and XANES spectroscopy, through photoelectron scattering, are structural probes of atomic positions, they are ideal methods to study variations of the local structure of proteins in solution. EXAFS spectroscopy has been applied to identify possible differences between Fe sites of low-affinity and high-affinity human hemoglobins in the deoxy state (28). No variation of the average Fe–N_p (where N_p is a pyrrole nitrogen) distance has been found, within the EXAFS error of 0.02 Å, and this experiment was considered as giving evidence of no variation of the Fe displacement out of the porphyrin plane in the two deoxy conformations. However, if the Fe moves from outside the heme plane into the heme plane with the $T_d \rightarrow R_d$ transition, keeping the same Fe–N_p distance, this displacement could not be detected by EXAFS spectroscopy. We have used XANES spectroscopy, which is sensitive to variations of bonding angles, to determine the variation of the local structure with the $T_d \rightarrow R_d$ transition in carp deoxyhemoglobin in solution.

MATERIALS AND METHODS

Carp blood was obtained as described (1). The packed cells, after washing, were kept under liquid nitrogen. To achieve lysis, 2.5 volumes of 0.1 mM Tris·HCl (pH 8) was added. After 1 hr, 0.1 M NaCl was added to the lysate, and the mixture was centrifuged at 15,000 rpm in a Sorvall SM24 rotor for about 20 min to remove the stroma. Then the samples were passed first through a Sephadex G-25 column equilibrated with 1 mM Tris·HCl (pH 8) and then through a Dintzis (36) deionizing column.

In order to obtain samples of deoxyhemoglobin, oxyhemoglobin was deoxygenated by continuous flushing with nitrogen gas and by adding dithionite under nitrogen flux. Carp deoxyhemoglobin in the R_d state was obtained by adding 0.07 ml of Tris buffer (pH 8.2) to 0.6 ml of deoxyhemoglobin solution under nitrogen flux. Carp deoxyhemoglobin in the T_d state was obtained by adding 0.07 ml of [bis(2-hydroxyethyl)amino]tris(hydroxymethyl)methane (Bistris) buffer (pH 6.2) and 0.02 ml of 200 mM Ins-P_6 to 0.6 ml of deoxyhemoglobin solution under nitrogen flux. The final hemoglobin concentration of the samples was about 10 mM. The R_d and T_d samples were prepared a few minutes before each experiment and kept always under anaerobic conditions. The two samples were put in two small cells (2 mm thick) with Mylar windows in the sample chamber for x-ray absorption measurements under helium atmosphere and at fixed temperature (15°C). The deoxy state was verified by optical spectra recorded with a Cary 219 spectrophotometer, and the transition from the low-affinity form at pH 6.2 to the high-affinity form at pH 8.2 was checked by the decrease of the Soret maximum at 430 nm. The experiment was repeated in six different runs over 2 years. In order to identify possible small differences between the spectra of the T_d and R_d samples, they were taken one after the other and the difference spectra were obtained.

The XANES measurements were performed at the Frascati "wiggler" facility, using synchrotron radiation monochomatized with a Si(111) channel-cut crystal. The spectra were collected by a transmission method. The threshold energy of the Fe edge has been defined as the first maximum of the derivative of the metal iron K edge. The absorption background due to excitations of lower binding-energy levels was subtracted in all spectra by polynomial fitting of the pre-edge region. The obtained spectrum due to core excitations from the Fe(1s) level has been normalized to the atomic absorption coefficient at high energy beyond the absorption jump $\alpha(E)/\alpha_{a\infty}$ obtained by linear fitting in the EXAFS region. When the data are plotted in this way, the iron absorption jump edge $\Delta\alpha_0$ is the unit of the reported absorption coefficient. An accurate normalization procedure is necessary to extract unambiguous variations of relative intensities of the XANES peaks. The energy resolution was about 1 eV, and energy shifts of absorption spectral features as low as 0.2 eV could be detected. A good signal-to-noise ratio ($\Delta\alpha = \pm 0.005\ \Delta\alpha_0$) was obtained by reaching very good stability of the electron beam in the storage ring and in the wiggler magnetic field.

RESULTS

Observed XANES Spectra

Fig. 1 shows the x-ray absorption spectra of carp deoxyhemoglobin in the low-affinity (T_d) and high-affinity (R_d) states over the XANES range and the beginning of the EXAFS oscillations. In Fig. 2 are the XANES spectra, over an enlarged scale, of carp deoxyhemoglobin in the R_d and T_d states and of human adult deoxyhemoglobin. In Fig. 3 are the spectra of carp deoxyhemoglobin in the T_d and R_d states compared with the oxygenated carp hemoglobin in ligated conformation, called here R_l.

The spectrum of human adult deoxyhemoglobin and the spectrum of the low-affinity carp deoxyhemoglobin (T_d) are identical within the sensitivity of our experiment. To analyze the subtle differences between the spectra of the T_d and R_d states of carp deoxyhemoglobin shown in Fig. 2, we obtained the difference spectrum. We can detect variations in the absorption coefficient as small as $5 \times 10^{-3}\ \Delta\alpha_0$, where $\Delta\alpha_0$ is the Fe K-edge absorption jump. The maximal variation of the absorption induced by the $T_d \rightarrow R_d$ transition is $\approx 3 \times 10^{-2}$, and it occurs about 15 eV above the Fe K edge. Moreover, we observe a blue shift of 0.2 ± 0.2 eV in the carp deoxyhemoglobin R_d spectrum, which is at the limit of experimental energy-shift sensitivity. We repeated the experiment several times and on different samples, but the same

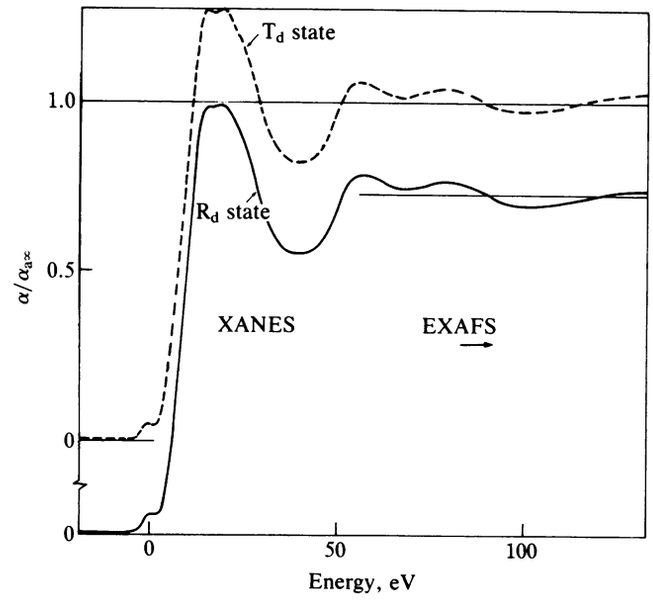

FIG. 1. X-ray absorption spectra at the Fe K edge of carp deoxyhemoglobin in the T_d quaternary conformation (dashed line) and in the R_d conformation (solid line) in the XANES full multiple scattering region and in the intermediate region at the beginning of EXAFS oscillations.

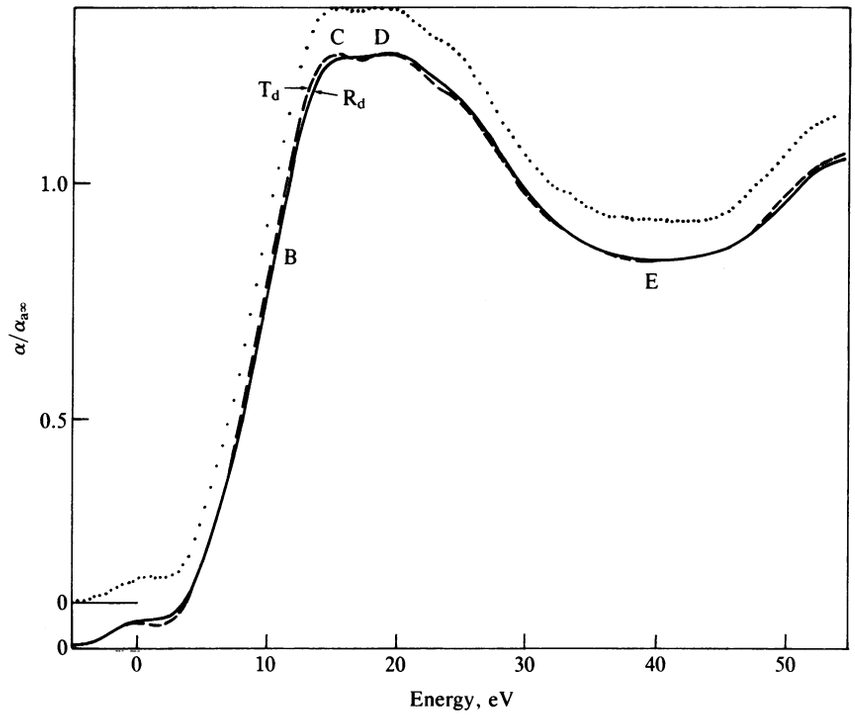

FIG. 2. XANES spectra (enlarged scale) of the T_d (dashed line) and R_d (solid line) forms of carp deoxyhemoglobin and of human adult deoxyhemoglobin (dotted line).

differences between R_d and T_d forms were detected in all runs.

To determine whether the observed variation might be due to the formation of a small quantity of methemoglobin in our sample, we simulated the modifications of the XANES spectra of deoxyhemoglobin (T_d) by adding 3% of the Fe K-XANES spectrum of methemoglobin to 97% of the Fe XANES spectrum of the carp deoxyhemoglobin at low pH (T_d). We found the same changes as in the spectra reported in Fig. 2. Therefore, we deduce that the spectra remain the same, within experimental error, in the two states.

A large variation in the Fe XANES spectrum is observed by going to the ligated state (Fig. 3). In fact, the absorption rising edge (or absorption jump edge) is shifted by 3.5 eV toward higher energy, and the line shape is quite different.

Theoretical XANES Spectra

We calculated the theoretical Fe K-XANES of hemoglobin by using the full multiple scattering theory (19, 20, 22). In this approach, the photoabsorption cross section W_c for one-electron transition from a core level at energy E_c to a state in

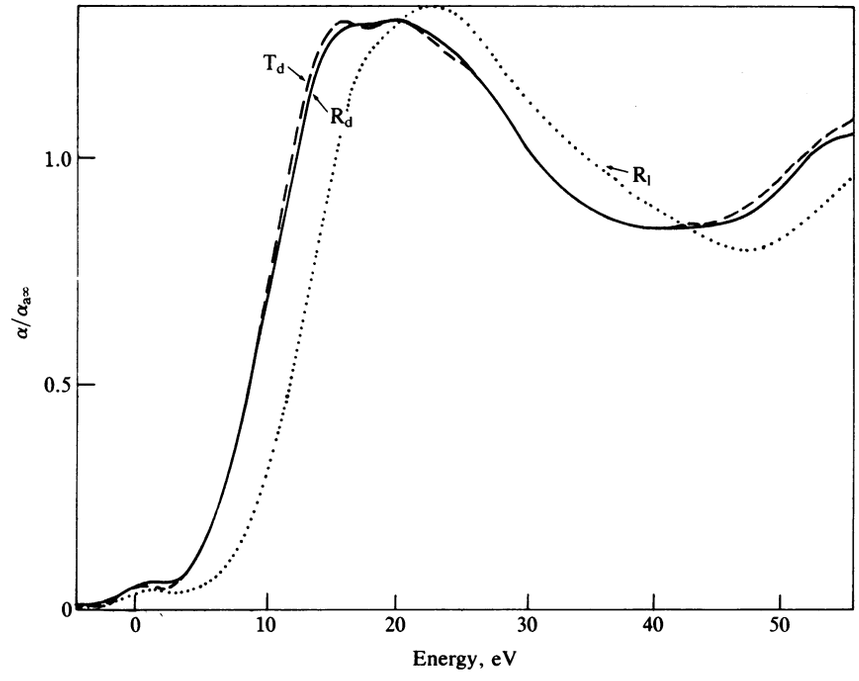

FIG. 3. The spectrum of carp oxygenated hemoglobin (dotted line) in the R_l state is reported with the spectra of carp deoxyhemoglobin in the R_d and T_d states.

the continuum at energy $E = E_c + \hbar\omega$ is calculated in a real-space multiple-scattering formalism:

$$W_c(\hbar\omega) = -2\Sigma_{LL'} m_L(E)\mathrm{Im}[\tau_{LL'}(E)]m^*_{L'}(E)\theta(E - E_f),$$

where E_f is the Fermi level; L stands for the pair (l, m) angular momentum numbers; $m_L(E)$ is the dipole matrix element, which is an atomic quantity; and $\tau_{LL'}$ is a real-space element of the full multiple-scattering matrix that gives the sum of all scattering paths for a photoelectron of energy E that begin and end on the Fe site. This $\tau_{LL'}$ matrix contains all the scattering effects of the surrounding atoms and produces the corresponding modulations of the absorption cross section. This method uses the "muffin-tin" form (17) for the potential of each atom.

We have made XANES calculations for a cluster of 30 atoms, with the Fe at the center and the nearest atoms of the porphyrin and of the proximal histidine. We have used the coordinates of human deoxyhemoglobin given by a recent crystallographic experiment with synchrotron radiation (29). The values of the averaged coordinates of atoms in the porphyrin plane were used to construct an idealized symmetrical porphyrin. This cluster has been classified as model b. Using these coordinates, we have obtained the spectrum shown in Fig. 4 (model b), which is in good agreement with the experimental spectrum of carp deoxyhemoglobin in the T_d form (Figs. 2 and 3).

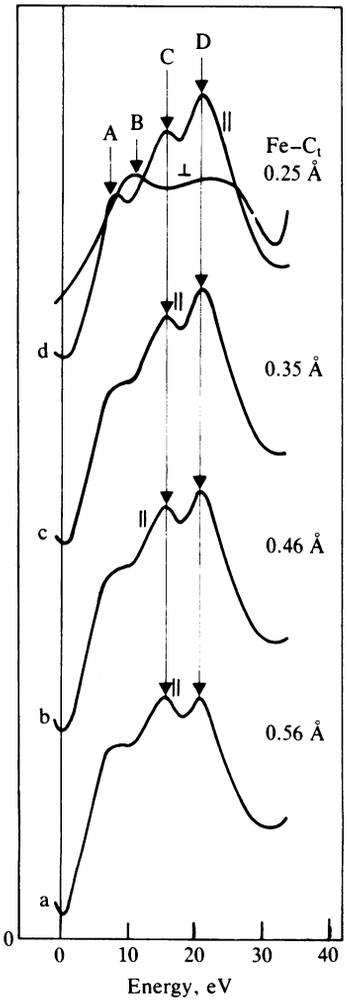

FIG. 4. Theoretical XANES calculations for a set of cluster models (a–d) where the porphyrin plane is kept fixed and the Fe is moved toward the plane. Fe–C_t indicates the distance between Fe and the center of porphyrin nitrogens. Polarized spectra with the electric vector of photons in the heme plane (||) and perpendicular to it (⊥) are plotted.

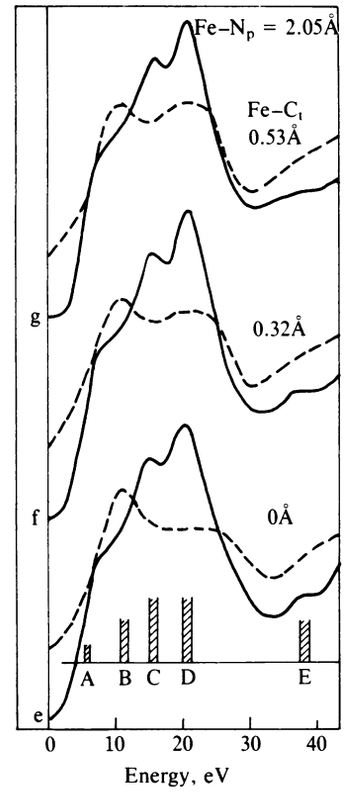

FIG. 5. Theoretical XANES calculations for a set of cluster models (*e–g*) are shown. Polarized spectra for the polarization vector in the heme plane (solid line) and perpendicular to it (dashed line) are shown. Fe is moved from the porphyrin plane (model e) to out-of-plane, accompanied by the tilting of the pyrroles of the heme in such a way that the Fe–N_p direction lies in the plane of the respective pyrrole. The spectral features from A to E at indicated energies can be identified.

The use of the coordinates of human hemoglobin (23, 24) is justified because the spectrum of carp deoxyhemoglobin in the T_d state is identical to the experimental XANES spectrum of human adult hemoglobin, as shown in Fig. 2. We performed XANES calculations for a set of clusters, b to d, by moving the Fe toward the center of porphyrin plane C_t and for b to a by moving Fe further away from the plane. The intensity of peak C clearly decreases with motion of Fe toward the heme plane from a position 0.5 Å out of the porphyrin plane. In this calculation the Fe–N_ε (nitrogen of proximal histidine F8) distance is kept fixed.

We performed XANES calculation for a set of models going from e to g (Fig. 5), where the Fe is in the porphyrin plane (model e) and it is moved out the plane with tilting of the pyrroles of the porphyrin toward the Fe, in such a way that Fe remains coplanar with each pyrrole. In this way the angles between Fe–N_p and the carbon atoms on each pyrrole remain constant. We found that the intensity ratio between peaks C and D does not change. However, comparison of the XANES of models a and g shows that the tilting of the pyrroles toward Fe out of plane reduces the intensity ratio C/D.

DISCUSSION

The energy blue shift of XANES features is expected for a contraction of interatomic distances. According with theoretical calculation of XANES (30, 31), a multiple scattering resonance at energy E moves to higher energy with decreas-

ing interatomic distance d following the rule $(E_r - E_b)d^2 = a$ constant, where E_b is the energy of a localized excitation at threshold, like the weak 1s→3d excitations at threshold of the XANES spectra of hemoglobins. The observed shift induced by oxygen binding in Fig. 3, which is the same as in human adult hemoglobin (32), is explained by XANES calculation as due to a contraction of 0.08 Å of the average Fe–N distance, which gives a shift of 1.8 eV and by chemical shift of about 1 eV of the Fe(1s) binding energy.

In the $T_d \rightarrow R_d$ transition there is no energy shift of the absorption jump edge larger than 0.2 eV; therefore, we interpret the data as indicating an upper limit of 0.01 Å for the Fe–N distance variations. This result is consistent with resonance Raman studies of carp deoxyhemoglobin. A shift [from 210 cm^{-1} to 216 cm^{-1} (13) or from 214 cm^{-1} to 223 cm^{-1} (14)] of the line assigned to the Fe–N_ε (His F8) stretching vibrational mode was found. This shift was assigned to a contraction of 0.008 Å of the Fe–N_ε bond in the $T_d \rightarrow R_d$ transition. In contrast, the Fe–N_p (pyrrole) stretching frequency remains unaltered upon the transition. Because we measure the variation of the average distance, such a small variation of the single Fe–N_ε distance is below the sensitivity of our method.

The decrease of the intensity of peak C relative to D has been observed in the comparison between deoxymyoglobin and adult human deoxy-HbA (23) and between fetal and adult deoxyhemoglobin (24), and it has been assigned to a different Fe displacement from the porphyrin nitrogen plane in the Fe 5-fold coordination geometry. Therefore, the variation of the intensity ratio between the peaks C and D is a measure of the displacement of the Fe out of the porphyrin plane. The calculated spectra reported in Fig. 4 for different Fe displacements show that this is the case. The theoretical and experimental (23, 24) results indicate that variations of the Fe displacement as small as 0.1 Å can be easily detected under our experimental conditions. That we did not observe variation of the intensity of the C/D ratio in the $T_d \rightarrow R_d$ transition indicates that there is no decrease of the Fe displacement larger than 0.1 Å.

The other possible effect due to the $T_d \rightarrow R_d$ transition is the "doming" of the heme, which would leave the Fe out-of-plane and the interatomic distances constant. The calculated spectra in Fig. 5 show that there is a large variation of the XANES spectrum in the presence of a large heme doming, with Fe displacement Fe–C_t = 0.5 Å (Fig. 5, model g), in comparison with the spectrum without doming and with the same Fe displacement (Fig. 4, model a). Therefore, we can exclude that the low- to high-affinity transition is accompanied by doming of the heme.

We have calculated the expected variations for the rotation of the proximal histidine around the normal to the heme plane. The results of the calculations show that this rotation leaves the XANES spectrum unaltered. Hence, this change of the local structure is not detected by XANES.

Our results show that the movement of Fe toward the plane (and the contraction of the Fe–N distance) in the $T_d \rightarrow R_d$ transition is not as suggested by the differences between the Fe site in deoxy-HbA crystal (29) and in oxy-HbA crystal (33), where there is a contraction of 0.08 Å of the Fe–N_p distance and movement from 0.4 Å out-of-plane into the porphyrin plane.

Our XANES studies on carp hemoglobin in solution show the following. (*i*) Although the affinities of the two carp deoxyhemoglobin forms T_d and R_d for oxygen differ, the change in quaternary structure that accompanies the $T_d \rightarrow R_d$ transition has no detectable effect on the heme. (*ii*) The Fe site structure is strongly modified by ligand binding. The Fe site structure in carp deoxygenated hemoglobin at high pH in the R_d (high-affinity) conformation is very different from the Fe site structure of carp oxygenated hemoglobin in the R_1 (high-affinity) conformation. Our work supplies positive evidence that the tertiary structure of carp deoxyhemoglobin is insensitive to the $T_d \rightarrow R_d$ transition, while within a given quaternary state the protein conformation is controlled by ligand binding in the sixth coordinate position. Our data suggest that the energy of cooperativity is stored away from the immediate heme environment, in agreement with recent results obtained by other experimental methods (34, 35).

We thank G. Fermi for discussions and for communication of the results of his experiment on deoxyhemoglobin before their publication and R. W. Noble for discussions and for providing carp hemoglobin.

1. Tan, A. L., De Young, A. & Noble, R. W. (1972) *J. Biol. Chem.* **247,** 2493–2498.
2. Noble, R. W., Parkhurst, L. J. & Gibson, Q. H. (1970) *J. Biol. Chem.* **245,** 6628–6633.
3. Parkhurst, L. J., Goss, D. J. & Perutz, M. F. (1983) *Biochemistry* **22,** 5401–5409.
4. Perutz, M. F. & Brunori, M (1982) *Nature (London)* **299,** 421–442.
5. Perutz, M. F. (1983) *Mol. Biol. Evol.* **1,** 1–28.
6. Perutz, M. F. (1970) *Nature (London)* **228,** 726–739.
7. Monod, J., Wyman, J. & Changeux, J. P. (1965) *J. Mol. Biol.* **12,** 88–101.
8. Nagai, K. & Kitagawa, T. (1980) *Proc. Natl. Acad. Sci. USA* **77,** 2033–2037.
9. Nagai, K., Kitagawa, T. & Morimoto, H. (1980) *J. Mol. Biol.* **136,** 271–289.
10. Desbois, A., Lutz, M. & Banerjee, R. (1981) *Biochim. Biophys. Acta* **671,** 177–183.
11. Ondrias, M. R., Rousseau, D. L. & Simon, S. R. (1982) *Proc. Natl. Acad. Sci. USA* **79,** 1511–1514.
12. Friedman, J. M., Rousseau, D. L., Ondrias, M. R. & Stepnoski, R. A. (1982) *Science* **218,** 1244–1246.
13. Dalvitt, C., Cerdonio, M., Fontana, A., Mariotto, G., Vitale, S., De Young, A. & Noble, R. W. (1982) *FEBS Lett.* **140,** 303–306.
14. Walters, M. A., Spiro, T. G., Scholler, D. M. & Hoffman, B. M. (1983) *J. Raman Spectrosc.* **14,** 162–165.
15. La Mar, G. N., Jue, T., Hoffman, B. M. & Nagai, K. (1984) *J. Mol. Biol.* **178,** 929–939.
16. Dalvitt, C., Miura, S., De Young, A., Noble, R. W., Cerdonio, M. & Chien, H. (1984) *J. Biochem. (Tokyo)* **141,** 255–259.
17. Bianconi, A. (1986) in *X Ray Absorption Principle: Applications Techniques of EXAFS, SEXAFS and XANES*, eds. Prinz, R. & Koningsberger, D. (Wiley, New York), pp. 167–174.
18. Bianconi, A., Incoccia, L. & Stripcich, S., eds. (1983) *EXAFS and Near Edge Structure* (Springer, Berlin).
19. Durham, P. J. (1986) in *X Ray Absorption Principle: Applications Techniques of EXAFS, SEXAFS, and XANES*, eds. Prinz, R. & Koningsberger, D. (Wiley, New York), pp. 164–166.
20. Durham, P. J. (1983) in *EXAFS and Near Edge Structure*, eds. Bianconi, A., Incoccia, L. & Stipcich, S. (Springer, Berlin), pp. 37–42.
21. Bianconi, A., Alema, S., Castellani, L., Fasella, P., Giovannelli, A., Mobilio, S. & Oesh, B. (1983) *J. Mol. Biol.* **165,** 125–138.
22. Durham, P. J., Pendry, J. B. & Hodges, C. R. (1982) *Comput. Phys. Commun.* **25,** 193–205.
23. Bianconi, A., Congiu-Castellano, A., Dell'Ariccia, M., Giovannelli, A., Durham, P. J., Burattini, E. & Barteri, M. (1984) *FEBS Lett.* **178,** 165–170.
24. Bianconi, A., Congiu-Castellano, A., Dell'Ariccia, M., Giovannelli, A., Burattini, E., Castagnola, M. & Durham, P. J. (1985) *Biochim. Biophys. Acta* **831,** 120–124.
25. Durham, P. J., Bianconi, A., Congiu-Castellano, A., Giovannelli, A., Hasnain, S. S., Incoccia, L., Morante, S. & Pendry, J. B. (1983) *EMBO J.* **2,** 1441–1443.
26. Bianconi, A., Congiu-Castellano, A., Durham, P. J., Hasnain, S. S. & Phillips, S. (1985) *Nature (London)* **318,** 685–687.
27. Congiu-Castellano, A., Bianconi, A., Dell'Ariccia, M., Giovannelli, A., Burattini, E. & Durham, P. J. (1984) in *EXAFS and Near Edge Structure*, Springer Proceedings in Physics, eds. Hodgson, K. O., Hedman, B. & Penner-Hann, J. E. (Springer, Berlin), Vol. 2, pp. 164–166.
28. Eisenberger, P., Shulman, R. G., Kincaid, B. M., Brown, G. S. & Ogawa, S. (1978) *Nature (London)* **274,** 165–170.
29. Fermi, G., Perutz, M. F., Shanaan, B. & Fourme, R. (1984) *J. Mol. Biol.* **175,** 159–174.
30. Bianconi, A., Dell'Ariccia, M., Gargano, A. & Natoli, C. R. (1983) *Springer Ser. Chem. Phys.* **27,** 57–61.
31. Bianconi, A., Fritsch, E., Calas, G. & Petiau, J. (1985) *Phys. Rev. B* **32,** 4292–4295.
32. Bianconi, A., Congiu-Castellano, A., Dell'Ariccia, M., Burattini, E. & Durham, P. J. (1985) *Biochem. Biophys. Res. Commun.* **131,** 98–102.
33. Shaanan, B. (1983) *J. Mol. Biol.* **171,** 31–59.
34. Rousseau, D. L. & Ondrias, M. (1985) *Biophys. J.* **47,** 537–545.
35. Friedman, J. M. (1985) *Science* **228,** 1273–1280.
36. Dintzis, H. M. (1953) Dissertation (Harvard Univ., Cambridge, MA).